



International Journal of Pharmacology

ISSN 1811-7775

science
alert

ansinet
Asian Network for Scientific Information



Research Article

Green Synthesized Silver Nanoparticle via *Cissus quadrangularis* as a Theranostic Agent for Colon Cancer

¹Chang Ge, ²Peng Wang, ¹Dehui Ji and ³Zhongkai Xu

¹Department of Anorectal Surgery, Central Hospital Affiliated to Shandong First Medical University, Jinan City, Shandong, 250013, China

²Department of General Surgery, The Second Affiliated Hospital of Shandong First Medical University, Tai'an City, Shandong, 271000, China

³Department of Gastrointestinal Surgery, Jinan Central Hospital, No. 105, Jiefang Road, Jinan City, Shandong, 250013, China

Abstract

Background and Objective: The green synthesis of the metallic nanoparticle by bioreduction is simple, economical, eco-friendly and cost-effective. Synthesis of metallic nanoparticles using plants contains several phytochemical compounds which are functionalized to nanoparticles. The main goal of this study is to synthesize silver nanoparticles using the aqueous extract obtained from the stem of *Cissus quadrangularis* and their anticancer activity on the HT29 colon cancer cell line. **Materials and Methods:** Silver nanoparticle was characterized by UV-visible spectroscopy, scanning electron microscopy, Fourier Transform Infrared (FTIR) spectroscopy etc. The cell viability and cytotoxicity of Ag-NP-CQ was confirmed by Trypan blue and MTT assay, in a dose-dependent manner. The apoptotic inducing ability of Ag-NP-CQ was investigated by ROS and NO estimation, propidium iodide staining and BAX and PARP gene expression by Polymerase Chain Reaction (PCR). **Results:** Results showed a greater reduction in viability of cells exposed and increasing cytotoxicity to green Ag-NP-CQ with increasing dose. Our data confirmed that Ag-NP-CQ enhances the antioxidant activity by scavenging the free radicals. Elevated apoptotic protein BAX with down regulated PARP was observed in Ag-NP-CQ treated cells regulates its anticancer effect through apoptotic signalling pathways. **Conclusion:** Based on the above findings biosynthesized silver nanoparticles with *Cissus quadrangularis* are very effective against colon cancer cell lines proving or exerting their anti-cancer activity.

Key words: Nanoparticles, *Cissus quadrangularis*, anticancer, HT29, antioxidant, apoptosis, scanning electron microscopy, Fourier transforms infrared spectroscopy

Citation: Ge, C., P. Wang, D. Ji and Z. Xu, 2022. Green synthesized silver nanoparticle via *Cissus quadrangularis* as a theranostic agent for colon cancer. Int. J. Pharmacol., 18: 1047-1057.

Corresponding Author: Zhongkai Xu, Department of Gastrointestinal Surgery, Jinan Central Hospital, No. 105, Jiefang Road, Jinan City, Shandong, 250013, China Tel: +8615668462595

Copyright: © 2022 Chang Ge *et al.* This is an open access article distributed under the terms of the creative commons attribution License, which permits unrestricted use, distribution and reproduction in any medium, provided the original author and source are credited.

Competing Interest: The authors have declared that no competing interest exists.

Data Availability: All relevant data are within the paper and its supporting information files.

INTRODUCTION

Colon cancer is one of the highly prevalent cancers around the world and claims a high number of lives. Globally, colon cancer remains the second leading in terms of mortality. In the year 2020 alone and 1.93 million cases of colon cancer have been diagnosed and 930,000 deaths have been recorded¹ and the mortality rate differs based on the available therapeutic options. According to GLOBOCAN database 2020, the occurrence of human colon cancer is 10.2% and the death rate has surged to 9.2%. This rise has resulted in making colon cancer the second cause of death worldwide. The incidence has increased potentially in several countries due to the adoption of Western dietary habits and lifestyles, which has been implicated in the risk of developing colon cancer². A current treatment strategy for colon cancer includes surgical excision of cancer, chemotherapy, radiation therapy and targeted therapy³. Non-targeted therapies cause a variety of side effects to include anaemia, gastrointestinal toxicity, mucositis, nausea, vomiting, hepatotoxicity, fatigue etc⁴. Targeted delivery using nanoparticles has gained much attention in recent times since nanoparticles provide a wide range of advantages over conventional treatment strategies⁵.

Plant extracts have been attempted to control colon cancer. *Cissus quadrangularis* is a vine that grows in Asia and Africa. The extract is used in traditional Chinese medicine, *Siddha* and *Ayurveda*. The extract from *C. quadrangularis* has been widely used for bone healing⁶. Apart from bone healing properties, the plant extract has been shown to possess antioxidant, anti-inflammatory, analgesic, anti-microbial activities⁷ has demonstrated weight loss by using *C. quadrangularis* extract in obese individuals. Further, the plant extract also has been shown to regulate metabolic syndrome⁸ extract from *C. quadrangularis* effectively inhibited the adipogenesis *in vitro*⁹ extract is also effective against cancer. Leukemic cells upon treatment with ethanolic and methanolic extracts of *C. quadrangularis* showed effective anti-cancer activity¹⁰. *Cissus quadrangularis* is found in tropical areas. The plant has been extensively used in *Ayurveda*, *Siddha* and Indian folk medicine to treat wound healing, heal bone fractures, correct menstrual irregularities. The plant extract has been shown to protect against male reproductive toxicity induced by a variety of pesticides and herbicides¹¹. Evidence is piling up suggestive of *Cissus quadrangularis* potential anti-cancer activity. Extract from *C. quadrangularis* is protective against skin cancer, cervical cancer, leukaemia cells etc^{12,13}.

Metal-based nanoparticles are gaining more attention for their rapid actions, unique physical and chemical properties.

Green synthesis of silver and gold nanoparticles is widely experimented with due to its flexible, reliable and prominent ions. AgNPs have been extensively explored for their cytotoxic potential¹⁴. It has been shown that plant (*Vitex negundo* L.) extract derived AgNPs are potent in inhibiting the proliferation of human colon cancer cells¹⁵. Based on the above findings, we synthesized silver nanoparticles synthesized using *C. quadrangularis* and evaluated their anti-cancer properties on colon cancer cell lines.

MATERIALS AND METHODS

Study area: This research was conducted in February, 2021, Department of Anorectal Surgery, Central Hospital Affiliated with Shandong First Medical University, Jinan city, Shandong, 250013, China.

Chemicals and reagents: Dulbecco's modified Eagle's medium, streptomycin, penicillin-G, L-glutamine, 3-(4,5 dimethylthiazol-2-yl)-2,5-diphenyltetrazolium bromide, phosphate-buffered saline, bovine serum albumin, Dimethyl Sulfoxide (DMSO), rhodamine-123, Ethylene Diamine Tetraacetic Acid (EDTA), triton X-100, 2',7'-diacetyl dichlorofluorescein, sodium dodecyl sulphate, trypan blue, trypsin-EDTA, acridine orange, ethidium bromide, ethanol were procured from Sigma Aldrich Chemicals Pvt. Ltd.

Collection of plant samples: The plant *Cissus quadrangularis* was collected in local areas in China. After excising leaves and tendrils and the plant samples were rinsed thoroughly to remove dirt with autoclaved water five times and sectioned into tiny pieces using a sterile scalpel under aseptic conditions as described by Ahmed *et al.*¹⁶. About 20 g of fresh leaves of *Cissus quadrangularis* was weighed and chopped into fine pieces and ground using mortar and pestle. The ground *Cissus quadrangularis* leaves were added to 100 mL of distilled water and boiled at 60 for 10 min using a microwave oven. After boiling, the extracts were allowed to reach room temperature. Finally, filtration of the extract was done with a what man No.1 filter paper (Hawach Scientific, Xi'an city, Shaanxi province, China).

Preparation of silver nanoparticle encapsulation with *Cissus quadrangularis*: The preparation of silver Nanoparticles was performed by a slight modification of Vanaja *et al.*¹⁷. A stock solution of silver nitrate (900 mL) having 5 mM concentration was prepared. The plant extract (*Cissus quadrangularis*) 100 mL was infused with a salt solution and the mixture was maintained at room temperature. After

24 hrs, the mixture was centrifuged at 8000 rpm for 10 min to separate the produced nanoparticles from the supernatant. The produced nanoparticles were dried in a hot air oven at 80°C and stored for further use. The dried nanoparticles were characterized using Fourier Transform Infrared (FT-IR). The spectra were recorded on a BRUKER spectrometer (Bruker Beijing scientific technology co., Ltd., Xixiaokou Road, Haidian District, China), between 400-4000 cm^{-1} . It was carried out to evaluate the presence of functional groups in the synthesized nanoparticles. Shape and surface morphology were identified using VEGA3TESCAN Scanning Electron Microscopy (SEM) TESCAN China, Ltd., Lianhang Road, Minhang District, Shanghai, China.

Cell culture: Human colon adenocarcinoma cancer HT29 cell line was procured from the Cell repository of ATCC. These cells were routinely grown in DMEM supplemented with 10% FBS. Penicillin (100 U mL^{-1})/streptomycin (100 $\mu\text{g mL}^{-1}$) antibiotic mixture was added to the medium to prevent bacterial contamination and they were maintained in an incubator supplied with 5% CO_2 at 37°C.

Morphometric analysis of HT-29 cells: The morphological changes of HT-29 colon cancer cells were checked under a phase-contrast microscope and the changes were recorded Moongkarndi *et al.*¹⁸. The cultured HT-29 cells were seeded (1×10^4 cells mL^{-1}) to 6 well plates and incubated for 24 hrs. After 24 hrs of incubation, different concentrations of Ag-NP-CQ were (10, 40, 70 and 100 $\mu\text{g mL}^{-1}$ added to the cells and control containing only HT29 cells and then were incubated in an atmosphere of 5% CO_2 at 37°C for 24 hrs. Followed by 24 hrs of treatment, the morphological changes were observed and taken pictures under a Phase contrast microscope (QUASMO optika microscope Biobase Meihua trading co Ltd., Jinan, Shandong, China). Cell treatment and control were kept in triplicates and the experiments were repeated thrice.

MTT assay: The cytotoxicity of Ag-NP-CQ extracts on HT29 cells was determined by the method of Sylvester¹⁹. For cell viability assay, briefly, HT29 viable cells were harvested and counted and then diluted using DMEM and seeded at a density of 1×10^4 cells in 100 μL medium for each well in 96-well plates and incubated for 24 hrs. After 24 hrs incubation, HT29 cells were checked for attachment using a microscope and treated with the different concentrations of Ag-NP-CQ (1-10 and 10-100 $\mu\text{g mL}^{-1}$) to each well. Treated HT29 cells were incubated at 37°C in a humidified incubator in an atmosphere of 5% CO_2 for 24 hrs. Post-incubation, the

drug-treated cells were washed with $1 \times \text{PBS}$ and the MTT (5 mg mL^{-1} in PBS) was added to each well and incubated for 4 hrs at 37°C. About 100 μL of DMSO was used to dissolve the formazan crystals formed. The cell viability was assessed by measuring the colour intensity at 540 nm using a multi-well plate reader (Microplate ELISA Reader, MPR-D111, Bioeuropeak, Jinan city, China). The results were expressed as a percentage of stable cells concerning the control. The half-maximal Inhibitory Concentration (IC_{50}) values were calculated and the optimum doses were derived by analyzing at various periods²⁰.

$$\text{Inhibition (\%)} = 100 - \frac{\text{Test OD}}{\text{Non-treated OD}} \times 100$$

The IC_{50} values were determined from the Ag-NP-CQ dose-responsive curve where inhibition of 50% cytotoxicity compared to control cells. Each concentration and control was maintained in triplicates and the experiment was repeated thrice.

Cell viability by trypan blue exclusion assay: The toxicity of nanoparticles on HT-29 cells was evaluated by trypan blue exclusion experiment Strober²¹. Cells were seeded in 6-well plates and treated with varying concentrations of Ag-NP-CQ (10-100 $\mu\text{g mL}^{-1}$) for 24 hrs of exposure in a humidified incubator (5% CO_2 , 37°C). Following incubation, the cells were trypsinized and resuspended in equal volumes of culture medium and trypan blue solution. The number of viable (unstained) and nonviable (blue-stained) cells were recorded using a hemocytometer to calculate the relative proportion of living and dead cells.

Measurement of Reactive Oxygen Species (ROS): The NBT reduction assay was performed for the estimation of ROS with slight modifications²² 1×10^5 cells mL^{-1} seeded and incubated for 24 hrs. Test samples Ag-NP-CQ (40, 70 and 100 $\mu\text{g mL}^{-1}$) were then added into the appropriate wells and incubated for 24 hrs. After incubation, the cells were washed with PBS twice followed by the addition of 100 μL of 0.1% NBT solution to each well of the 24 hrs incubated cells. Roughly after 1 hr, the medium was carefully removed and the cells were washed with 70% methanol three times. About 120 μL of 2 M potassium hydroxide (KOH) was added to the dried well followed by the addition of 120 μL of DMSO to each well. Absorbance was recorded in a microplate reader at 630 nm with KOH/ DMSO as blank.

Measurement of Nitric Oxide (NO): HT-29 colon cancer cells were maintained in DMEM supplemented with 10% FBS,

streptomycin (50 µg mL⁻¹) and penicillin (50 U mL⁻¹) at 37°C in an atmosphere of 5% CO₂. After reaching 80-90% confluency, the cells were washed with PBS and trypsinized, centrifuged at 120 rpm at 4°C for 10 min. The cell suspension was made with a density of 2 × 10⁶ cells mL⁻¹. Care was taken to maintain cell viability of more than 90% as determined by the trypan blue exclusion assay. Cells were seeded in a 96 well plate at a density of 4 × 10⁵ cells/well in a volume of 50 µL well⁻¹. The plate was incubated at 37°C, in an atmosphere of 5% CO₂ to enhance cell attachment. Different concentrations of the Ag-NP-CQ (40, 70 and 100 µg mL⁻¹) were added and they were maintained in the incubator. Cells were further incubated for 24 hrs and Griess assay for nitrite determination using the spent media as described by Wahyuni *et al.*²³.

Sulfanilamide solution and NED solution were equilibrated at room temperature for around 20 min and 50 µL of each culture supernatant was added to 96-well plate in triplicates. Culture supernatant was added with 1% sulfanilamide in 5% phosphoric acid (50 µL) followed by incubation at room temperature for 5-10 min in dark. All the wells were added with 50 µL of the 0.1% NED solution and maintained at room temperature for 10 min in dark. The plate was observed for the appearance of purple/magenta colour within 30 min and absorbance was recorded in a plate reader with a filter range of 520 and 550 nm. The values were compared against the standard curve and the corresponding value was determined.

Measurement of apoptosis by Propidium Iodide (PI) staining: Apoptotic cells were detected by fluorescence microscopy by method Du *et al.*²⁴. The control and treated (40, 70 and 100 µg mL⁻¹) HT-29 colon cancer cells were incubated 30 min in the dark with 50 µg mL⁻¹ PI. The suspended cell lines were washed with PBS and then analyzed by fluorescence microscopy. Excessive PI was removed by washing the adherent cells with PBS followed by harvesting the cells by standard trypsinization (0.5 mg mL⁻¹ trypsin and 0.2 mg mL⁻¹ EDTA in PBS, Sigma). Detached cells were collected as suspension and pelleted by centrifugation and washed again with PBS to remove PI before fluorescence microscopy.

Gene expression by the polymerase chain reaction

DNA isolation: Cells were recovered by trypsinization followed by centrifugation for 5 min at 1200 rpm. The cells were washed in 1 mL of ice-cold PBS and recovered by centrifugation. 1 volume of digestion buffer was added to the cell pellet and resuspended. For approximately <3 × 10⁷ cells,

0.3 mL of digestion buffer was used. The samples were incubated at 50°C for 12-18 hrs in tightly capped tubes. After incubation, an equal volume of phenol-chloroform-isoamyl alcohol (25:24:1) was added and mixed. The mixture was then centrifuged at 3000 rpm for 5 min at room temperature. The aqueous phase was mixed with ½ the volume of 7.5 M ammonium acetate and twice the volume of absolute ethanol was added, mixed well and centrifuged at 3000 rpm for 5 min at room temperature. The pellet was washed 70% ethanol. After air drying, the pellet was dissolved in 30 L nuclease-free water. The isolated DNA was used for PCR.

Gene expression analysis

Primers: β-Actin, BAX and PARP primers were used. Nucleotide sequence alignments of BAX and PARP genes were obtained through databases. Based on these alignments, BAX primers (forward -5'CGTGTCTGATCAATCCCCGA 3') and (Reverse -5'GAGGCCAGAAGGCAGGATTG 3') genes were designed, PARP (forward -5'CCCAGCCTTGTGGAAAACAC 3') and (Reverse -5'CACCTGCAGAGACAGGCATT 3') genes were designed.

PCR: The annealing temperature for each primer set was optimized using thermal cycler gradient PCR (Hangzhou Bioer Technology Co., Ltd., Hangzhou, Zhejiang, China). The volume of the total reaction mixture was 25 µL with 50 ng templates DNA, 1 × PCR Emerald master mixture, 1 µM each of forward and reverse primer and 1.5 U Taq polymerase. Following is the amplification program: 1 cycle at 95°C for 5 min for initial denaturation. 35 cycles of 95°C for 1 min for DNA denaturation, 54°C (β-Actin), 56°C (PARP) and 54.3°C (BAX) for 30 sec for annealing and 72°C for 1 min for extension of two strands. The final extension was carried out at 72°C for 5 min. The PCR products were analyzed on a 1.0% agarose gel incorporated with ethidium bromide and visualized under UV and photographed.

RESULTS

Characterization of biosynthesized AgNPs

SEM: The Scanning Electron Microscope (SEM) was used to characterize the morphology of nanoparticles. The data of Fig. 1 shows the SEM images of the prepared biosynthesized silver (Ag) nanoparticles.

FTIR: FTIR spectrum Fig. 2 of the *C. quadrangularis* inspired silver nanoparticles shows different IR bends absorbed at 2981.54 cm⁻¹ denoted C-H stretching alkene compound, 2488.36 cm⁻¹-NH₂ amines, 1018.09 cm⁻¹-C-N stretch aliphatic

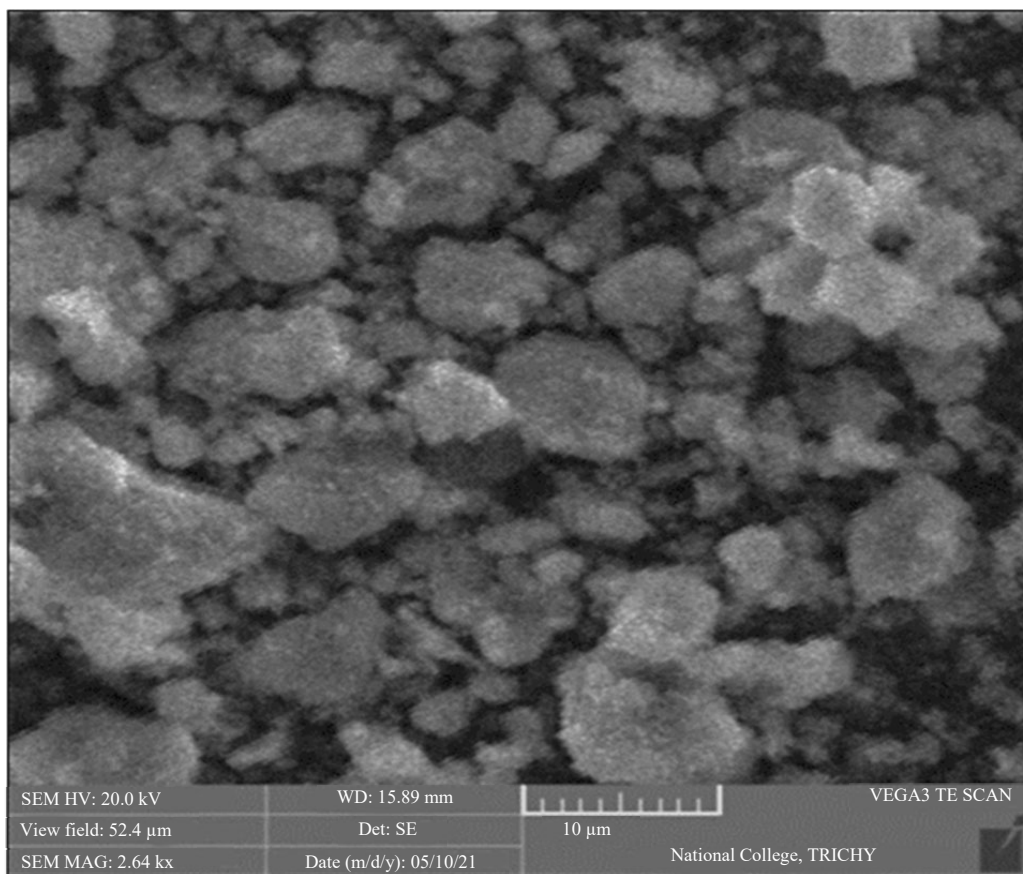


Fig. 1: Formation of silver nanoparticles and their presents in aggregated form
Scanning Electron Microscope (SEM) was used to characterize the morphology of nanoparticles

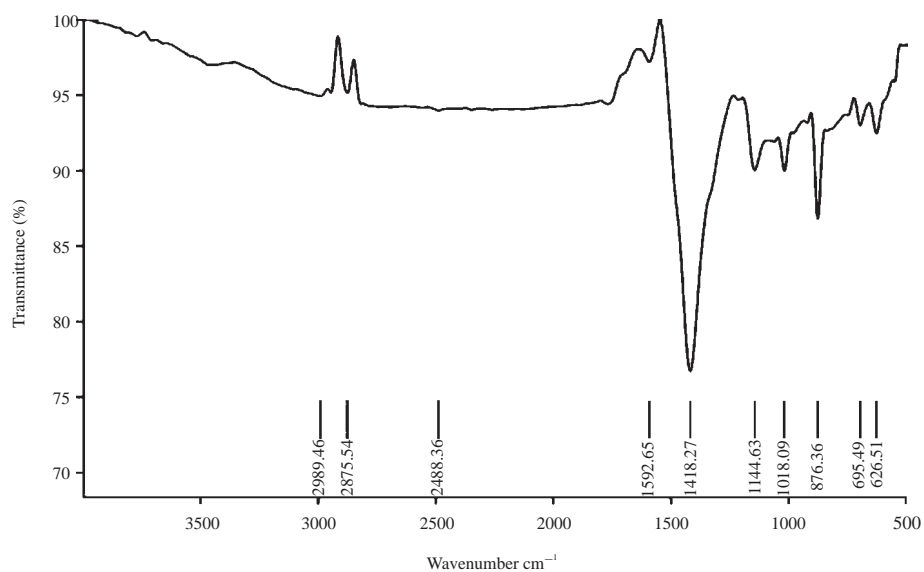


Fig. 2: FTIR spectrum of the *Cissus quadrangularis* derived SNPs
Dried nanoparticles were characterized using Fourier Transform Infrared (FT-IR). The spectra were recorded on a BRUKER spectrometer between 400-4000 cm^{-1} . It was carried out to evaluate the presence of functional groups in the synthesized nanoparticles

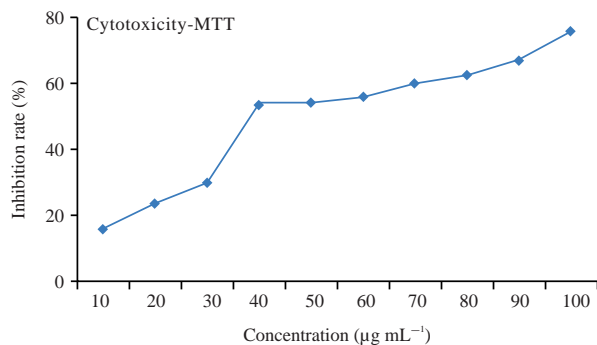


Fig. 3: LC₅₀ range of the sample was found at 40 µg mL⁻¹ concentration, whereas the toxicity of the cell was 75% at 100 µg mL⁻¹ concentration

amines, 1144.63 cm⁻¹-C-O stretch alcohols, 1418.27 cm⁻¹ -OH bend carboxylic acid, 876.36 cm⁻¹ strong C-CL stretch halo compounds, respectively.

Cytotoxicity assay-MTT: MTT assays were performed to determine the cellular metabolic activity as an indicator of cell viability. Cytotoxicity of the biosynthesized SNPs to find the effective dose for its anticancer activity assessment using MTT assay. The yellow tetrazolium salt (3-(4,5-dimethylthiazol-2-yl)-2,5-diphenyltetrazolium bromide or MTT) to purple formazan crystals were formed by metabolically active cells and dense purple colour is directionally proportional to the number of viable cells and they were quantified by using a multiwell spectrophotometer at 500-600 nm absorbance. The biosynthesized silver nanoparticle with *Cissus quadrangularis* was added to human colon cancer HT-29 cells. Followed by the 24 hrs treatment, cells were replaced with MTT reagent and read under Microplate ELISA Reader, MPR-D111, Bioevopeak, Jinan city, China) and the results were showing the dose-dependent inhibition of the cell growth and based on these results the IC₅₀ value of the biosynthesized silver nanoparticle of *Cissus quadrangularis* was selected (Fig. 3).

Cell viability assay: Live and dead cells were analyzed using trypan blue dye for the assessment of cell viability. Trypan blue dye stained the nuclei of the dead cells, which is used to analyse the cytotoxicity of the drugs. In this present study, human colon HT-29 cells were treated with Ag-NP-CQ for 24 hrs with different concentrations (10, 40, 70 and 100 µg mL⁻¹). Followed by trypsinization, cells were washed with 1×PBS and then collected and counted and added trypan blue dye and counted under a light microscope Bioevopeak Co., Ltd., Jinan, Shandong, China. The dye excluded the live cells and stains to the dead cells were

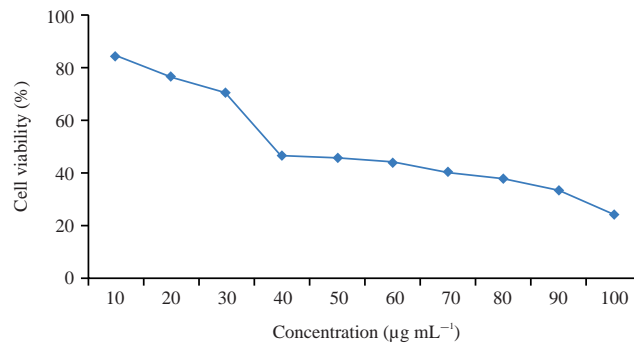


Fig. 4: Effect of biosynthesized SNPs on cell viability of HT29 cell line

observed in a dose-dependent manner. Based on the cell viability the IC₅₀ values were noted at the concentration of 40 µg mL⁻¹, where 50% of cells were stained (Fig. 4).

Morphometric analysis: Morphological changes are the important signature of the cancer cells. While cancer cells grow it multiplies the cell number as well as changes in their appearances which can be used to identify the best target for the drug development. Anticancer drugs are developing programmed cell death thereby inducing the cells to undergo stress which reveals the membrane blebbing, floating cells, rounded cells. The *Cissus quadrangularis* treated human Colon cancer HT29 cells for 24 hrs showed morphological changes in a dose-dependent manner. The HT-29 colon cancer cells were incubated with different concentrations of biosynthesized silver nanoparticles of *Cissus quadrangularis* (10, 40, 70 and 100 µg mL⁻¹). After 24 hrs incubation cells underwent membrane shrinkage and detached and visualized under phase-contrast microscopy, which is the typical characteristic of apoptosis. We have noted the high toxicity was induced at the dose of 70 and 100 µg mL⁻¹. The dose of 40 µg mL⁻¹ showed 50% inhibition of the cells (Fig. 5a-d).

Apoptosis assay: The phase-contrast microscopic results revealed and indicated the occurrence of apoptosis (Fig. 6a-d) i.e., rounded, detached cells, Membrane blebbing and apoptotic bodies in Ag-NP-CQ treated cells. The anticancer effect of the drugs induces apoptosis is programmed cell death and the present study showed the apoptosis induction after 24 hrs treatment of biosynthesized nanoparticle with *Cissus quadrangularis* in human colon cancer HT29 cells. The propidium iodide staining showed the bright red condensed or blebbing nucleus is an indication of apoptosis and it was visible in Ag-NP-CQ treated cells when compared with control cells and showed maximum condensed nucleus.

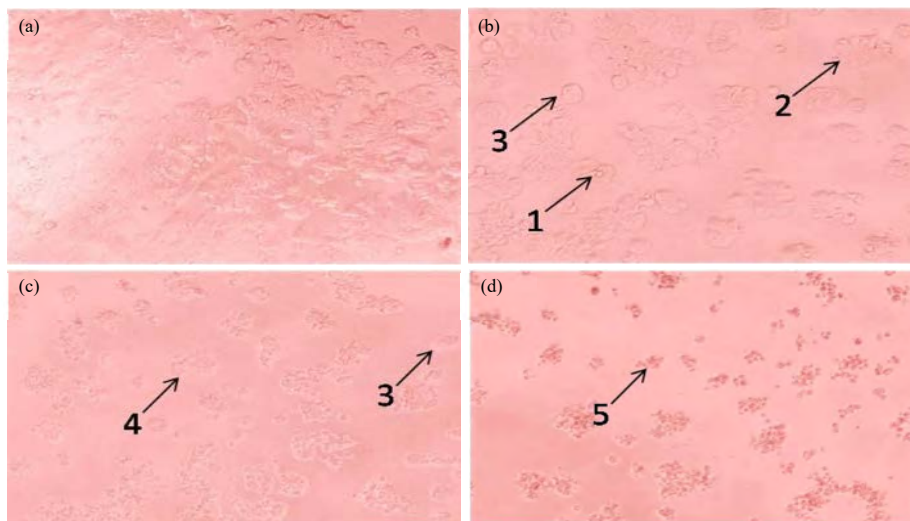


Fig. 5(a-d): Morphometric analysis of the cancer cells, (a) Control, (b) $40 \mu\text{g mL}^{-1}$, (c) $70 \mu\text{g mL}^{-1}$ and (d) $100 \mu\text{g mL}^{-1}$ *Cissus quadrangularis* treated human Colon cancer HT29 cells for 24 hrs showed morphological changes in a dose-dependent manner

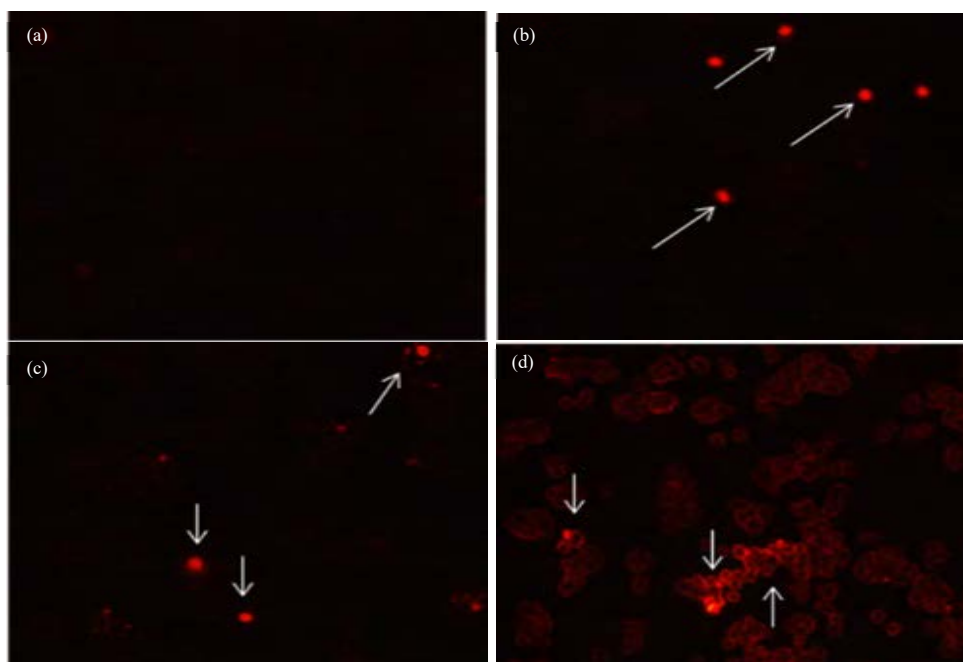


Fig. 6(a-d): Apoptosis assay of the cancer cells, (a) Control, (b) $40 \mu\text{g mL}^{-1}$, (c) $70 \mu\text{g mL}^{-1}$ and (d) $100 \mu\text{g mL}^{-1}$ Phase-contrast microscopic results revealed and indicated the occurrence of apoptosis (Fig. 4) i.e., rounded, detached cells, membrane blebbing and apoptotic bodies in Ag-NP-CQ treated cells. Arrow mark (\rightarrow) represents the apoptotic cells

Measurement of Reactive Oxygen Species (ROS): Reactive Oxygen Species (ROS) production were measured qualitatively using the NBT method. The Ag-NP-CQ treated HT-29 human colon cancer cells accumulated reactive oxygen species were seen in a dose-dependent increase within the cells (Fig. 7).

Measurement of Nitric Oxide (NO): HT29 cells treated with the biosynthesized *Cissus quadrangularis* silver nanoparticle as control, 40, 70 and 100 μL for 24 hrs. NO (Nitric acid) production was significantly increased with the increasing sample concentration (Fig. 8).

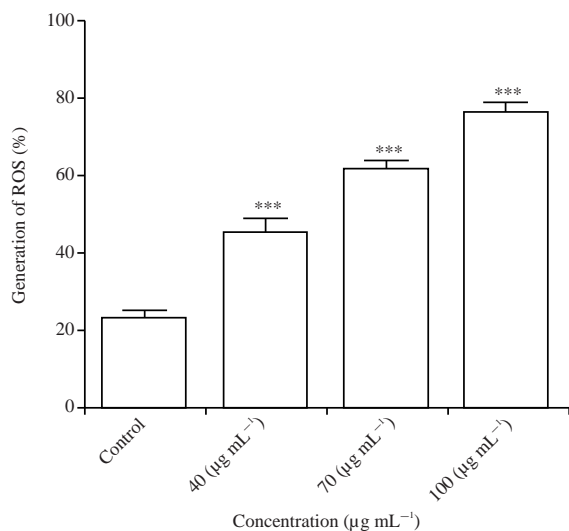


Fig. 7: HT29 cells treated with the biosynthesized *Cissus quadrangularis* silver nanoparticle as control, 40, 70 and 100 µL for 24 hrs

ROS production was significantly increased with the increasing sample concentration. Sample values are expressed as the (Mean ± SD) of the results of 3 independent experiments (n = 3). Significant difference ***p<0.0001 compared with the untreated control, as determined by a one-way ANOVA with the Tukey multiple-comparison post test

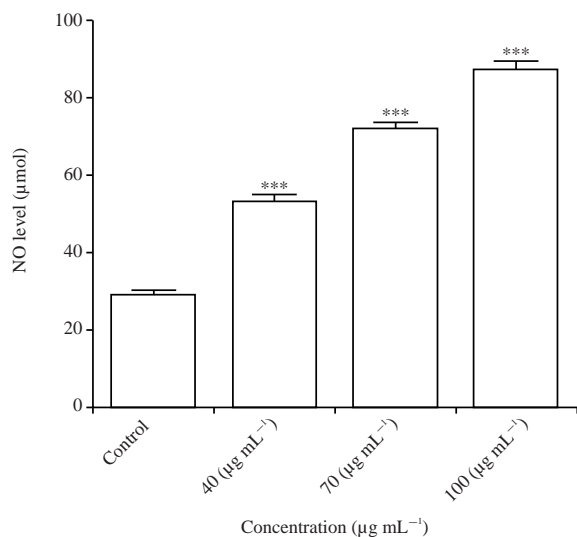


Fig. 8: HT29 cells treated with the biosynthesized *Cissus quadrangularis* silver nanoparticle as control, 40, 70 and 100 µL for 24 hrs.

NO (Nitric acid) production was significantly increased with the increasing sample concentration. Sample values are expressed as the (Mean ± SD) of the results of 3 independent experiments (n = 3). Significant difference ***p<0.0001 compared with the untreated control, as determined by a one-way ANOVA with the Tukey multiple-comparison post test

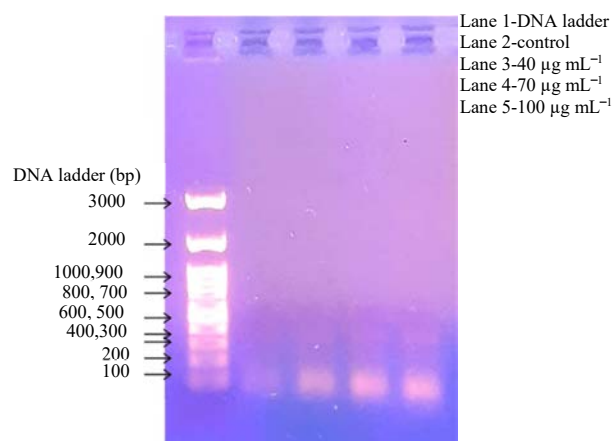


Fig. 9: Apoptotic gene BAX was up regulated gene expression

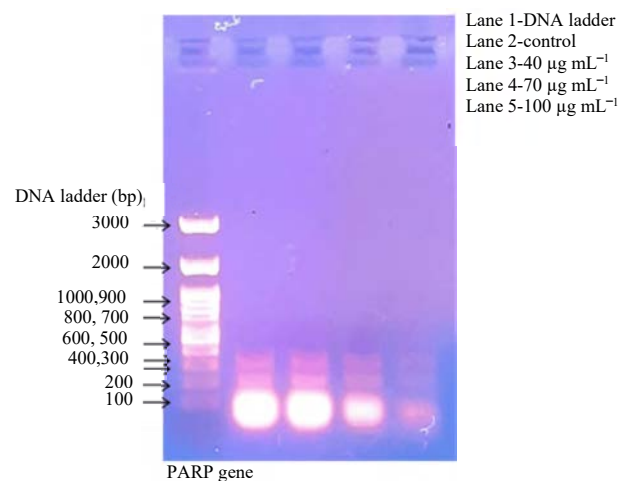


Fig. 10: Anti-apoptotic gene was down regulated gene expression with Ag-NP-CQ in a dose-dependent manner

PCR gene analysis of BAX and PARP: Gene expression analysis were conducted by PCR for the assessment of anti-cancer activity and induction of apoptosis using gene-specific primers. In this study, we have examined two genes BAX and PARP both genes involved in apoptotic gene signalling pathways and play an important role in signalling mechanisms in cancer cells. After 24 hrs treatment with biosynthesized silver nanoparticles of *Cissus quadrangularis* inhuman Colon cancer, HT29 cells were processed for PCR gene analysis. The apoptotic BAX was up regulated (Fig. 9) and on the other hand PARP, an anti-apoptotic gene was down regulated (Fig. 10) with Ag-NP-CQ in a dose-dependent manner.

DISCUSSION

Therefore, in the current work, we evaluated the anti-cancer potential of silver nanoparticles synthesized using the extract of *C. quadrangularis* on the colon cancer cell. We used the HT-29 cell line to assess the anti-cancer activity of the green synthesized silver nanoparticle.

Cytotoxicity assay revealed that *C. quadrangularis* derived silver nanoparticles showed an LC₅₀ at a concentration of 40 µg mL⁻¹ (Fig. 3). The cell survival was showing an opposite trend. The survival of cells declined progressively beyond the calculated LC₅₀ (40 µg mL⁻¹). Our results are in line with the previous observations^{10,12,13}. The plant extract has been shown to induce mitochondrial-mediated apoptosis which is triggered by ROS induced by the plant extract Sheikh *et al.*²⁵. The plant extract is known to modulate ROS effectively. In male reproductive toxicity, the extract causes reduce the ROS whereas in cancer cells it causes an increase in ROS. It remains elusive how *Cissus quadrangularis* modulates ROS in different cell lines differently. However, our cytotoxic assays suggest that *C. quadrangularis* is anti-proliferative in HT-29 colon cancer cell lines. Anti-proliferative effect combined with the potential to induce apoptosis would be the ideal property of an anti-cancer agent.

To analyze if the *C. quadrangularis* derived silver nanoparticles induce apoptosis morphological changes were observed. We observed the following morphological changes in cells which include rounding of cells, shrinkage of cells, membrane blebbing, pyknotic bodies and apoptotic bodies which are typical of cells undergoing apoptosis. The aforementioned changes were well pronounced at higher concentrations of the nanoparticle (Fig. 5a-d). To further confirm apoptosis we performed PI staining. Staining with propidium iodide is one of the gold standards for the confirmation of apoptosis²⁶. A dose-dependent increase in apoptotic bodies was observed in PI stained images confirming the involvement of apoptosis by *C. quadrangularis*-derived silver nanoparticles. Figure 6a-d Earlier reports also suggest that *C. quadrangularis* induces apoptosis in cancer cells¹².

The evidence from the literature suggests that induction of ROS could be one of the mechanisms of apoptosis induction in cancer cells²⁵. To evaluate the involvement of ROS in inducing apoptosis, HT-29 cells were treated with varying concentrations of *C. quadrangularis* derived silver nanoparticles and quantified ROS. There was a dose-dependent increase in the amount of ROS (Fig. 7). Earlier studies have shown that the expression of IGFBP4 could

mediate apoptosis in cancer cells²⁷. Therefore, it could be possible that the *C. quadrangularis* derived silver nanoparticles could have induced IGFBP4 to induce apoptosis. On the other hand, ROS induces DNA damage and result in cell cycle arrest. An especially double-strand break causes genotoxicity²⁸. Earlier studies also suggest that ROS mediated upregulation of Bcl-2 is one of the mechanisms of inducing apoptosis in cancer cells²⁹. STATs are upstream of ROS induction by having control over mitochondrial membrane permeability³⁰. Earlier studies have revealed that ROS triggers G2/M arrest by modulating the MAPK pathway. Similarly, in our experiment also biosynthesized nanoparticles could have also played a role in inducing apoptosis via MAPK pathway and cell cycle arrest.

Nitric oxide is one of the highly reactive toxic gases which has free access into any subcellular compartment owing to its ability to pass through any type of membrane system. Because of its deleterious effects on the cellular processes, it is widely accepted for its anti-cancer potential³¹. NO has also been shown to have an inhibitory effect on cancer metastasis³². Therefore, we evaluated NO in HT-29 cells upon treatment with *C. quadrangularis* loaded silver nanoparticles. Surprisingly, there was a significant dose-dependent increase in the concentration of silver nanoparticles. NO has well been established to inhibit autophagy and promote apoptosis in hepatocellular carcinoma. Nitric oxide inhibits autophagy and promotes apoptosis in hepatocellular carcinoma. NO also inhibits pro-survival factors such as NFκB³³, have discussed extensively the role of NO in nanomaterial mediated cancer therapeutics. Overall, it is apparent that NO-induced by the *C. quadrangularis* loaded silver nanoparticles could have a stronger role inducing in cytotoxicity of cancer cells³⁴.

As *C. quadrangularis* effective in activating PARP to induce apoptosis, we quantified the expression PARP by PCR. Our results indicated that the expression of PARP is decreased in a dose-dependent manner. Figure 10 PARP is a protein involved in repairing DNA damage and therefore is essential for maintaining genomic stability. Earlier studies suggest that NO is involved in inducing PARP³⁵. Several As the nanoparticles suppress the expression of PARP DNA repair would likely be adversely affected. The NO, on one hand, induces genomic toxicity and on the other hand, suppresses the DNA repairing activity leading to cell cycle arrest and apoptosis.

BAX is a protein that is involved in disrupting the membrane potential of the mitochondria and contributes to apoptosis. We evaluated the expression of BAX by PCR. Upon treatment of colon cancer cell line with *C. quadrangularis*

loaded silver nanoparticles the expression of BAX in the cells increased in a dose-dependent manner. Earlier studies suggest that ROS induces the phosphorylation of BAX which leads to apoptosis of cancer cells³⁶. Similarly, in our study also, ROS induced by the *C. quadrangularis* loaded silver nanoparticles could have phosphorylated BAX to cause apoptosis.

CONCLUSION

In conclusion, our study reveals the anti-cancer potential of *C. quadrangularis* loaded silver nanoparticles against colon cancer. *C. quadrangularis* has been shown to have several medicinal properties. The biosynthesized silver nanoparticles caused cytotoxicity against cancer cells and inhibited cell viability. The nanoparticles caused apoptosis of the cancer cells which was evidenced by PI staining and by morphological changes of the cancer cells. Further, the particles increased ROS and NO levels in the cancer cells. At the molecular level, there was a decrease in the expression of PARP. ROS and NO causes DNA damage and genotoxicity. As PARP is inhibited the DNA repair is halted aggravating genotoxicity which could have caused cell cycle arrest and subsequently apoptosis which is confirmed by the increased expression of BAX. Overall, from our studies, it is evident that *C. quadrangularis* loaded silver nanoparticles are effective against colon cancer.

SIGNIFICANCE STATEMENT

The current study explores the possibility of *C. quadrangularis* loaded silver nanoparticles to treat colon cancer. The nanoparticles are effective in inducing apoptosis in colon cancer cells *in vitro* as suggested by nuclear condensation and membrane blebbing. Further, these nanoparticles elevate ROS and NO within the colon cancer cells which result in genotoxicity which is further aggravated by inhibition of DNA repair mechanisms. Cell cycle arrest combined with apoptosis restricts the cancer progression as suggested by the expression levels of BAX. Our study, strongly emphasizes the potential of *C. quadrangularis* loaded silver nanoparticles against colon cancer.

REFERENCES

1. Ferlay, J., M. Colombet, I. Soerjomataram, D.M. Parkin, M. Piñeros, A. Znaor and F. Bray, 2021. Cancer statistics for the year 2020: An overview. *Int. J. Cancer*, 149: 778-779.
2. Vernia, F., S. Longo, G. Stefanelli, A. Viscido and G. Latella, 2021. Dietary factors modulating colorectal carcinogenesis. *Nutrients*, Vol. 13. 10.3390/nu13010143.
3. Tang, X., Y. Liang, X. Feng, R. Zhang, X. Jin and L. Sun, 2015. Co-delivery of docetaxel and poloxamer 235 by PLGA-TPGS nanoparticles for breast cancer treatment. *Mater. Sci. Eng.: C*, 49: 348-355.
4. Ades, S., 2009. Adjuvant chemotherapy for colon cancer in the elderly: Moving from evidence to practice. *Oncology*, Vol. 23.
5. Banerjee, A., S. Pathak, V.D. Subramaniam, G. Dharanivasan, R. Murugesan and R.S. Verma, 2017. Strategies for targeted drug delivery in treatment of colon cancer: Current trends and future perspectives. *Drug Discovery Today*, 22: 1224-1232.
6. Singh, P., A. Gupta, I. Qayoom, S. Singh and A. Kumar, 2020. Orthobiologics with phytoactive cues: A paradigm in bone regeneration. *Biomed. Pharmacother.*, Vol. 130. 10.1016/j.biopha.2020.110754.
7. Stohs, S.J. and S.D. Ray, 2013. A review and evaluation of the efficacy and safety of *Cissus quadrangularis* extracts. *Phytother. Res.*, 27: 1107-1114.
8. Oben, J., D. Kuate, G. Agbor, C. Momo and X. Talla, 2006. The use of a *Cissus quadrangularis* formulation in the management of weight loss and metabolic syndrome. *Lipids Health Dis.*, Vol. 5. 10.1186/1476-511X-5-24.
9. Lee, H. J., B. Le, D.R. Lee, B.K. Choi and S.H. Yang, 2018. *Cissus quadrangularis* extract (CQR-300) inhibits lipid accumulation by downregulating adipogenesis and lipogenesis in 3T3-L1 cells. *Toxicol. Rep.*, 5: 608-614.
10. Dhanasekaran, S., 2020. Phytochemical characteristics of aerial part of *Cissus quadrangularis* (L) and its *in-vitro* inhibitory activity against leukemic cells and antioxidant properties. *Saudi J. Biol. Sci.*, 27: 1302-1309.
11. Kokilavani, P., U. Suriyakalaa, P. Elumalai, B. Abirami, R. Ramachandran, A. Sankarganesh and S. Achiraman, 2014. Antioxidant mediated ameliorative steroidogenesis by *Commelina benghalensis* L. and *Cissus quadrangularis* L. against quinalphos induced male reproductive toxicity. *Pestic. Biochem. Physiol.*, 109: 18-33.
12. Bhujade, A., G. Gupta, S. Talmale, S.K. Das and M.B. Patil, 2013. Induction of apoptosis in A431 skin cancer cells by *Cissus quadrangularis* Linn stem extract by altering Bax-Bcl-2 ratio, release of cytochrome c from mitochondria and PAPR cleavage. *Food Funct.*, 4: 338-346.
13. Siddiqui, S., Q. Zia, M. Abbas, S. Verma and A. Jafri *et al.*, 2021. Antiproliferative activity of *Cissus quadrangularis* L. extract against human cervical cancer cells: *In vitro* and *in silico* analysis. *Anticancer Agents Med. Chem.*, Vol. 21. 10.2174/1871520621666210210103729.

14. Huy, T.Q., P.T.M. Huyen, A.T. Le and M. Tonezzer, 2020. Recent advances of silver nanoparticles in cancer diagnosis and treatment. *Anti-Cancer Agents Med. Chem.*, 20: 1276-1287.
15. Prabhu, D., C. Arulvasu, G. Babu, R. Manikandan and P. Srinivasan, 2013. Biologically synthesized green silver nanoparticles from leaf extract of *Vitex negundo* L. induce growth-inhibitory effect on human colon cancer cell line HCT15. *Process Biochem.*, 48: 317-324.
16. Ahmed, S., Saifullah, M. Ahmad, B.L. Swami and S. Ikram, 2016. Green synthesis of silver nanoparticles using *Azadirachta indica* aqueous leaf extract. *J. Radiation Res. Applied Sci.*, 9: 1-7.
17. Vanaja, M., G. Gnanajobitha, K. Paulkumar, S. Rajeshkumar, C. Malarkodi and G. Annadurai, 2013. Phytosynthesis of silver nanoparticles by *Cissus quadrangularis*: Influence of physicochemical factors. *J. Nanostruct. Chem.*, Vol. 3. 10.1186/2193-8865-3-17.
18. Moongkarndi, P., N. Kosem, S. Kaslungka, O. Luanratana, N. Pongpan and N. Neungton, 2004. Antiproliferation, antioxidation and induction of apoptosis by *Garcinia mangostana* (mangosteen) on SKBR3 human breast cancer cell line. *J. Ethnopharmacol.*, 90: 161-166.
19. Sylvester, P.W., 2011. Optimization of the Tetrazolium Dye (MTT) Colorimetric Assay for Cellular Growth and Viability. In: *Drug Design and Discovery*, Satyanarayanajois, S.D. (Ed.), Humana Press, pp: 157-168.
20. Shahneh, F.Z., S. Valiyari, A. Azadmehr, R. Hajiaghaee, S. Yaripour, A. Bandehagh and B. Baradaran, 2013. Inhibition of growth and induction of apoptosis in fibrosarcoma cell lines by *Echinophora platyloba* DC: *In vitro* analysis. *Adv. Pharmacol. Sci.*, Vol. 2013. 10.1155/2013/512931.
21. Strober, W., 2015. Trypan blue exclusion test of cell viability. *Curr. Protocols Immunol.*, Vol. 21. 10.1002/0471142735.ima03bs21.
22. Zhang, H.J., W. Zhao, S. Venkataraman, M.E.C. Robbins, G.R. Buettner, K.C. Kregel and L.W. Oberley, 2002. Activation of matrix metalloproteinase-2 by overexpression of manganese superoxide dismutase in human breast cancer MCF-7 cells involves reactive oxygen species. *J. Biol. Chem.*, 277: 20919-20926.
23. Wahyuni, F.S., D.A.I. Ali, N.H. Lajis and Dachriyanus. 2017. Anti-inflammatory activity of isolated compounds from the stem bark of *Garcinia cowa* Roxb. *Pharmacogn. J.*, 9: 55-57.
24. Du, J., C. Chen, Y. Sun, L. Zheng and W. Wang, 2015. Ponicidin suppresses HT29 cell growth via the induction of G1 cell cycle arrest and apoptosis. *Mol. Med. Rep.*, 12: 5816-5820.
25. Sheikh, S., S. Siddiqui, A. Dhasmana, Safia and E. Haque *et al.*, 2015. *Cissus quadrangularis* Linn. Stem ethanolic extract liberates reactive oxygen species and induces mitochondria mediated apoptosis in KB cells. *Pharmacogn. Mag.*, 11: 365-374.
26. Riccardi, C. and I. Nicoletti, 2006. Analysis of apoptosis by propidium iodide staining and flow cytometry. *Nat. Protocols*, 1: 1458-1461.
27. Wei, W., L. Wang, L. Xu and J. Zeng, 2021. Anticancer mechanism of breviscapine in non-small cell lung cancer A549 cells acts via ROS-mediated upregulation of IGFBP4. *J. Thoracic Dis.*, 13: 2475-2485.
28. Srinivas, U.S., B.W.Q. Tan, B.A. Vellayappan and A.D. Jeyasekharan, 2019. ROS and the DNA damage response in cancer. *Redox Biol.*, Vol. 25. 10.1016/j.redox.2018.101084.
29. Jin, Y.Z., H.N. Sun, Y. Liu, D.H. Lee and J.S. Kim *et al.*, 2019. Peroxiredoxin V inhibits emodin-induced gastric cancer cell apoptosis via the ROS/Bcl2 pathway. *In Vivo*, 33: 1183-1192.
30. Wang, Y., X. Yu, H. Song, D. Feng, Y. Jiang, S. Wu and J. Geng, 2018. The STAT-ROs cycle extends IFN-induced cancer cell apoptosis. *Int. J. Oncol.*, 52: 305-313.
31. Hirst, D. and T. Robson, 2010. Nitric oxide in cancer therapeutics: Interaction with cytotoxic chemotherapy. *Curr. Pharm. Des.*, 16: 411-420.
32. Xie, K. and S. Huang, 2003. Contribution of nitric oxide-mediated apoptosis to cancer metastasis inefficiency. *Free Radical Biol. Med.*, 34: 969-986.
33. Bauer, J.A., J.A. Lupica, J.A. Didonato and D.J. Lindner, 2020. Nitric oxide inhibits Nf- κ B-mediated survival signaling: Possible role in overcoming TRAIL resistance. *Anticancer Res.*, 40: 6751-6763.
34. Seabra, A.B. and N. Durán, 2015. Nanotoxicology of metal oxide nanoparticles. *Metals*, 5: 934-975.
35. Maciag, A.E., R.J. Holland, Y. Kim, V. Kumari and C.E. Luthers *et al.*, 2014. Nitric oxide (NO) releasing poly ADP-ribose polymerase 1 (PARP-1) inhibitors targeted to glutathione S-transferase P1-overexpressing cancer cells. *J. Med. Chem.*, 57: 2292-2302.
36. Quast, S.A., A. Berger and J. Eberle, 2013. ROS-dependent phosphorylation of Bax by wortmannin sensitizes melanoma cells for TRAIL-induced apoptosis. *Cell Death Dis.*, Vol. 4. 10.1038/cddis.2013.344.